

Asian Journal of Scientific Research

ISSN 1992-1454





Asian Journal of Scientific Research 6 (3): 555-563, 2013 ISSN 1992-1454 / DOI: 10.3923/ajsr.2013.555.563 © 2013 Asian Network for Scientific Information

Study of Physical and Mechanical Properties of Aluminum 6092/SiC_{25n}/t6 friction Stir Welded Plate

¹Umar Patthi, ¹Mokhtar Awang, ¹Faiz Ahmad, ¹Ahmad Majdi Abdul Rani, ²Norbert Ezinger and ²Andreas Hutter

Corresponding Author: Umar Patthi, Department of Mechanical Engineering, Universiti Teknologi PETRONAS, Bandar Seri Iskandar, 31750 Tronoh, Perak, Malaysia

ABSTRACT

Friction Stir Welding (FSW) is a relatively new joining technique and the application of the technique is still limited. Among the advantages of this method compared to the conventional welding techniques is that it reduces problem associated to metal re-solidification as the technique involves no melting stages. Such advantages are especially applicable for joining high strength aerospace material such as aluminium Metal Matrix Composite (MMC). In this study, the physical and mechanical properties of Friction Stir Welding (FSW) on aluminium 6092/SiC_{25p}T6 was discussed and established. Weld characteristic was analyzed using SEM, EDX and XRD, while mechanical properties were analyzed using Vickers hardness and tensile test. Weld microstructure observation shows distribution of fine and coarse particle cross the weld area. Microstructure analysis reveals difference in redistribution of particles between the zones in the weld area, which consist of the weld centre, advancing and retreating side of the tool. XRD results depict insignificant difference of post weld stresses as well as maintained material phases. The weld centre shows increase in hardness and an adequate retainment of the material strength. In conclusion FSW causes changes in the material microstructure due to the onset of plastic deformation and the post weld result shows it does retain or even improve some of the material properties.

Key words: Aluminum metal matrix composite, silicon carbide, weld, friction stir welding, microstructure, mechanical

INTRODUCTION

The use of Metal Matrix Composite (MMC) in today's industrial application is widespread. The unique properties of the material has attracted its usage mainly in the aerospace field application and recently it has been used in the automotive, transportation and as well as in the recreation industry (Maruyama, 1999). Manufacturers have utilize the materials in constructing bike body frame, car engine parts and the used of the material in constructing armour vehicle body parts.

The challenges in joining MMC material through conventional fusion welding processes is primarily related into retaining the material post weld properties. The onset of liquidation causes the migration of the reinforcement particle out from the weld nugget causing particle voids within the welding zone. Liquidation also promotes new phase changes which cause the material to lose

¹Department of Mechanical Engineering, Universiti Teknologi PETRONAS, Bandar Seri Iskandar, 31750 Tronoh, Perak, Malaysia

²Institute of Material Science and Welding, Mechanical Engineering and Economic Science, Graz University of Technology, Graz, Austria

its valuable properties within the weld nugget which is unwanted. Although some recent work proves that MMC can be adequately joined through normal fusion welding processes but the process still causes defects in the welding properties and microstructure (Storjohann *et al.*, 2003). To curb this, new joining methods were introduce in the MMC joining processes. One of these welding methods is friction stir welding where material can be joined without melting and without using filler material to promote joining. The objective of this paper is to establish physical and mechanical properties of friction stir welding on aluminum 6092/SiC_{25p}/T6.

MATERIALS AND METHODS

The type of material used for this work is aluminum 6092 plates reinforced with 25 volume percentage of SiC particulate. The thickness for the plate used for the welding is 12.7 mm. The material was produced by DWA Company based in California U.S.A.

Equipment and welding methods: In the first week of July 2011 FSW process was conducted by using a state of the art FSW-plant by MTS in Graz University of Technology. The machine has a bearing surface of 24501×1250 mm, maximum welding velocity of 6 m min⁻¹, engine maximum speed of 3200 rpm, maximum downward force of 35 kN and maximum torque of 180 Nm. A butt joint technique was used to join the two plates together. The rotational speed of the hardened tool during the FSW was held constant at 900 rpm and a traverse speed was held at 100 mm min⁻. The tool is tilted at 3° angle during its movement along the welding line. The type of material used for the fabrication of the tool is H13 tool steel. A tapered 10.16 mm tool pin length with 25 mm tool shoulder diameter was used for the joining process.

Analytical methods and equipments used: Metallographic observation was conducted to study the redistribution of the SiC particulates and also to detect other deformities that might have occurred during the welding processes. Cross section of the welded joint was characterized by using Scanning Electron Microscope (SEM), Energy-dispersive X-ray spectroscopy (EDX) and X-ray Diffraction (XRD). The sample surfaces were prepared by standard metallographic techniques. XRD was conducted to detect any changes in the space lattice (d-spacing) and also to detect any development of new phases within the material. Chemical composition analysis using spot EDX were also performed to confirm the elements within the weld segment and base metal.

Temperature history was recorded to analyze the temperature distribution during the welding process. The readings were then stored and displayed in a chart to see the temperature variation. K-type thermocouple probe was used in the temperature reading.

The material hardness was measured using Vickers hardness method with 200 g force. Tensile test was also done.

RESULTS AND DISCUSSION

Microstructure analysis: The joining of the composite material through friction stir welding was successfully accomplished. Weld cross section reveals that the two plates were welded perfectly without any visible defects. Typically in a FSW cross section, the area is divided into 4 separate zones, which are the base metal, Heat Affected Zone (HAZ), Thermo Mechanical Affected Zone (TMAZ) and the weld nugget (Awang *et al.*, 2011). The weld nugget could also be analyzed into 3 separate zones, which is the weld centre, Advancing Side (AS) and the retreating side (RS).

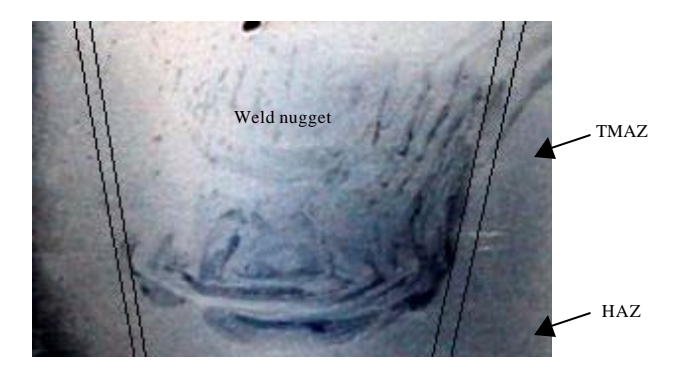


Fig. 1: A typical onion flow of the FSW cross sectioned sample

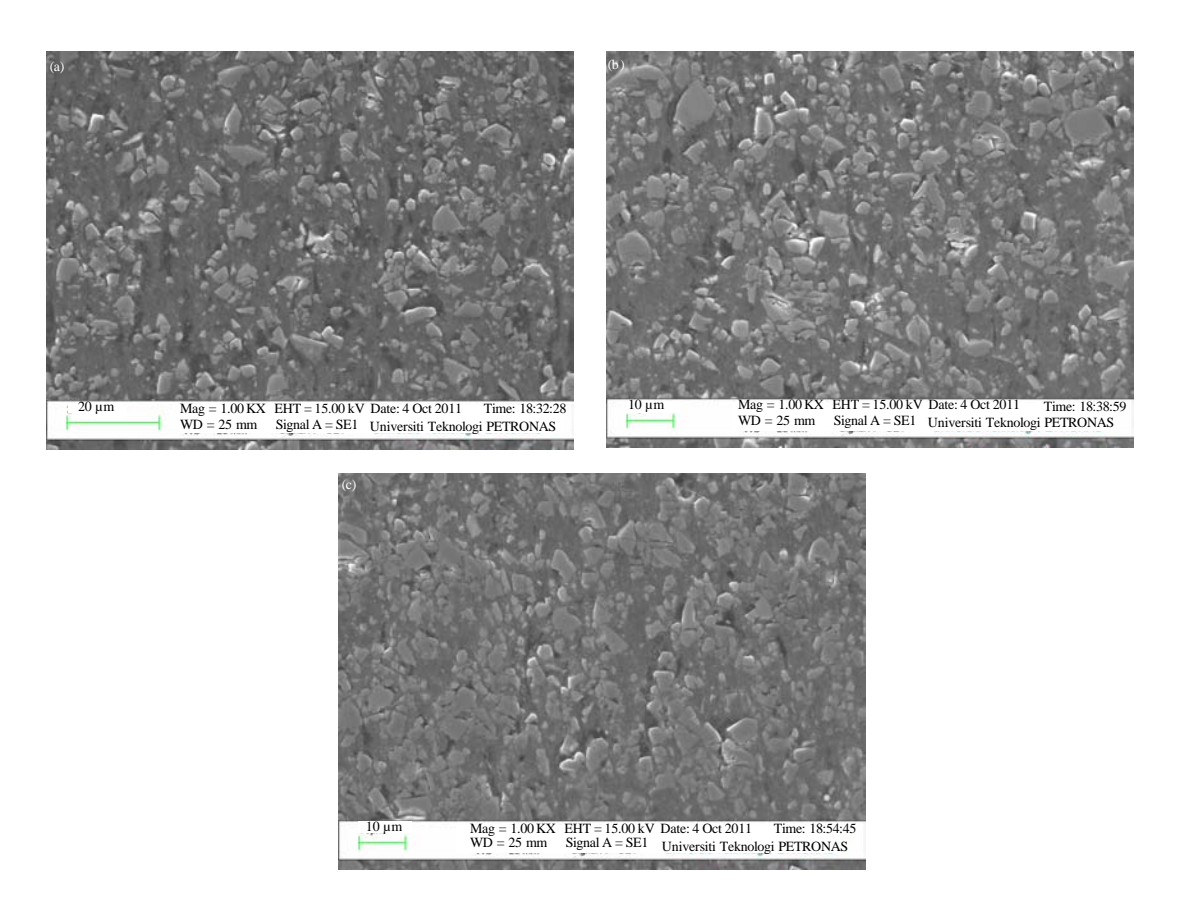


Fig. 2(a-c): FSW microstructure comparison for three different regions (a) Base metal, (b) TMAZ and (c) Weld nugget

Typical onion flow was observed on these kinds of welds (Fig. 1), which was caused by the material flow during the joining process (Storjohann *et al.*, 2003).

SEM micrograph in Fig. 2a shows the initial alignment and spread of the SiC particulate in the base metal. When compared to Fig. 2b through 2c (TMAZ region and the weld nugget), there is a

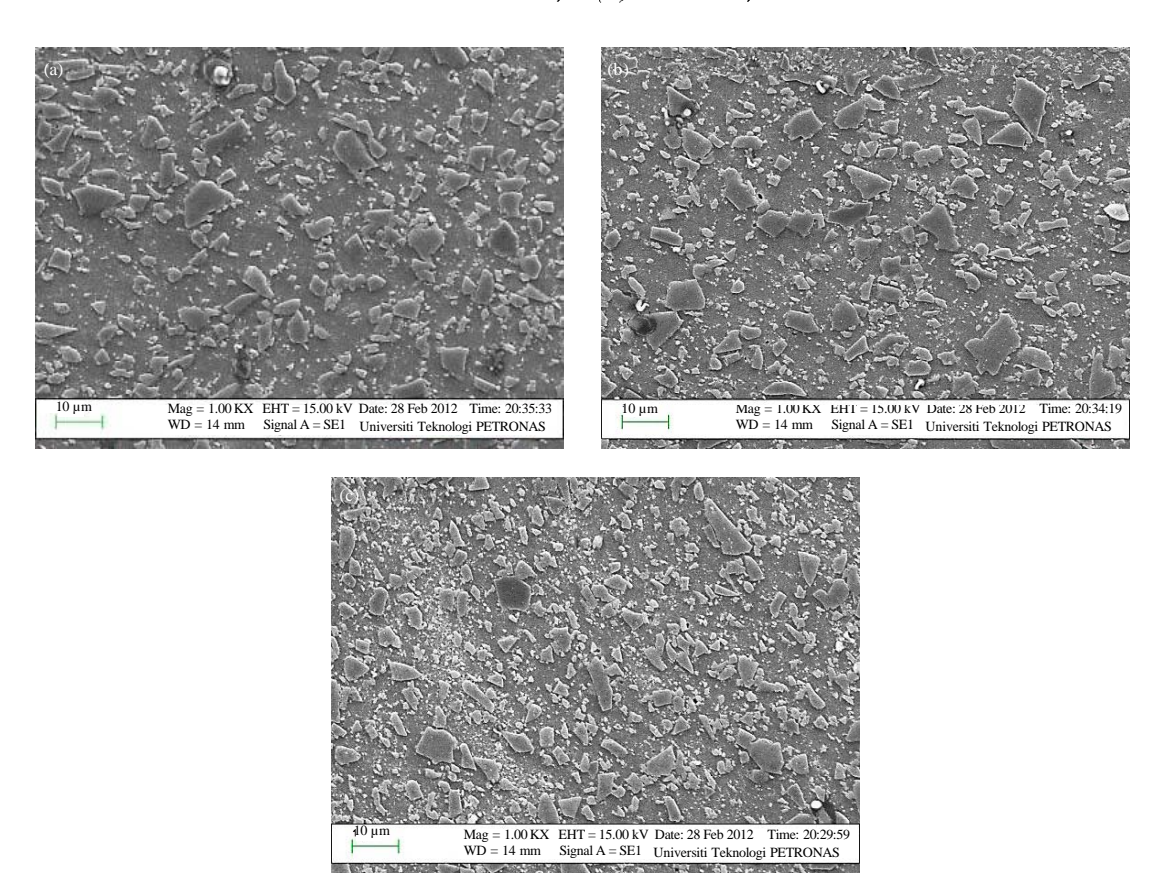


Fig. 3(a-c): SEM micrograph depicts the location of the silicon carbide (SiC) particle distribution within the (a) Retreating side, (b) Weld centre and (c) Advancing side of the weld nugget

significant case of SiC particulate realignment. It is observed from the SEM micrograph that there is a definite re-concentration of SiC particulate within the weld region, Fig. 2c. SEM observation in Fig. 2c shows a denser SiC particulate concentration within the weld nugget.

The SEM image in Fig. 2c illustrates that the weld nugget has a smaller and finer SiC particulate when compared to the other two regions (base metal and TMAZ). The coarse SiC particulates in the weld region are also rounder and smaller. This is due to knocking and chipping effect on the coarse SiC particulate during the high velocity stirring. SEM image in the weld nugget also depicts concentration of fine SiC particulate around the coarser SiC particulate. No dendritic structure is detected within the welded joint which is usually observed in fusion welding processes (Storjohann et al., 2005).

SEM micrograph in Fig. 3 further shows the distribution of SiC particulate within the weld nugget. SEM micrograph depicts an unsymmetrical spread of coarse and fine SiC particulate within the weld centre, advancing side and the retreating side of the weld (Root *et al.*, 2009). Images show a higher density of coarse SiC particulate in the retreating side (Fig. 3a) of the weld when compared to the weld centre and advancing side. The advancing side (Fig. 3c) exhibits a higher percentage of fine SiC particulate and more homogenous distribution of fine and coarse SiC particulate when compared to the other two regions.

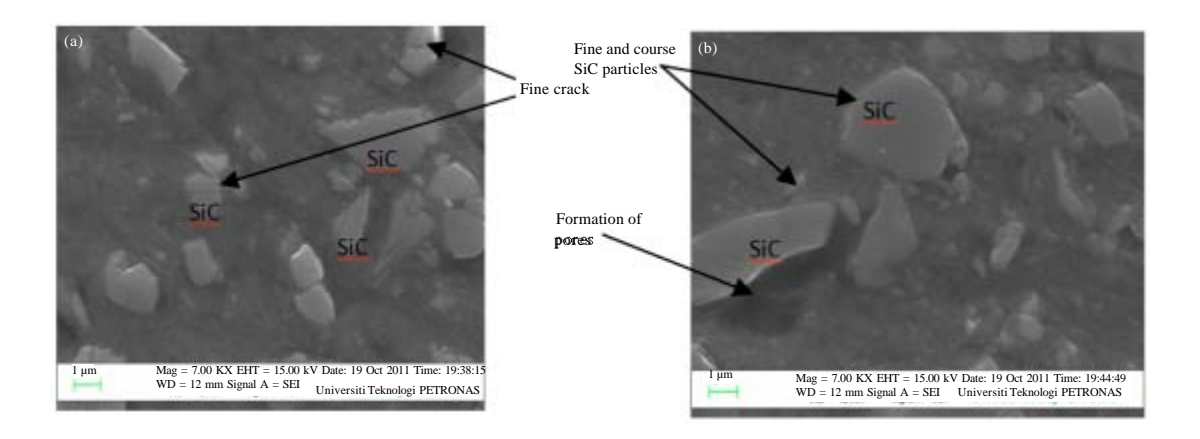


Fig. 4(a-b): A higher magnification of the weld nugget, (a) Depicts formation of fine cracks and (b)

Depicts formation of pores in the aluminum matrix

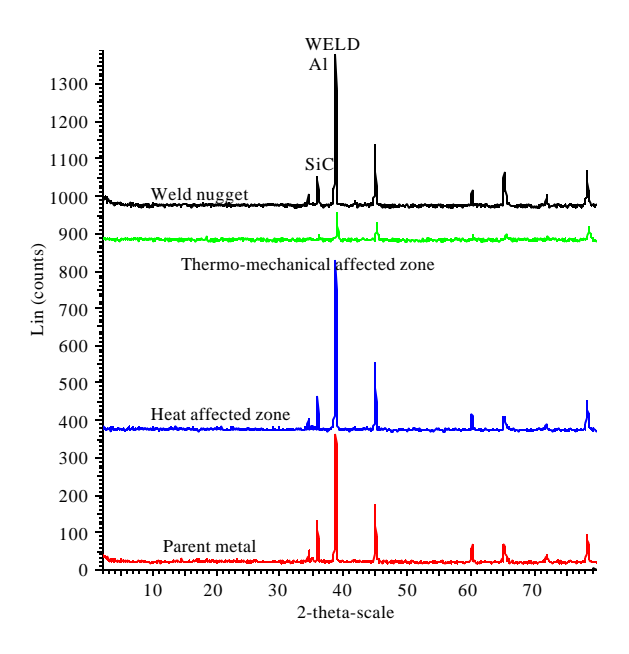


Fig. 5: Phase change evaluation (Patthi and Awang, 2011)

The high rate of stirring action causes formation of fine crack and rounding of coarse SiC particulate edges which was observed in the weld nugget in Fig. 4a. Based on Fig. 4b it can be observed that there were developments of pores at a certain side of the coarse SiC particle but it also shows that at other interfaces between the coarse SiC particle and the matrix that the bonding is quite intact. Intact interfaces between the SiC particulate and the aluminium alloy matrix are observed mainly on the fine SiC particulate. The formation of fine cracks and pores had also been reported by earlier work done on this subject (Uzun, 2007).

XRD analysis: Based on the XRD results (Fig. 5), there are no evidence of phase changes when comparing between base metal and the welded zones. This shows that the welding process does not

Table 1: D spacing analysis

| | D-spacing | |
|--------------|---------------|----------|
| Zones | | |
| Welding zone | Aluminum peak | SiC peak |
| Base metal | 2.32175 | 2.50602 |
| HAZ | 2.32636 | 2.50064 |
| TMAZ | 2.31261 | 2.48994 |
| Weld nngget | 2.32636 | 2.50602 |

(Patthi and Awang, 2011)

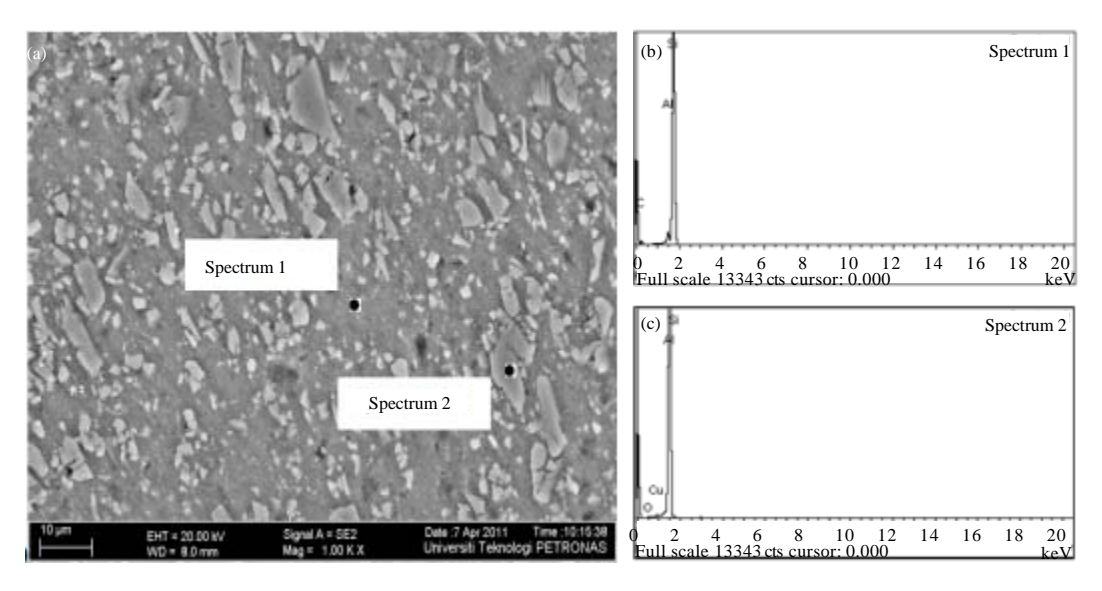


Fig. 6(a-c): (a) The location of the spot EDX spectrum 1 and 2 and EDX graph of, (b) SiC particulate element on spectrum 1 and (c) Aluminum matrix on spectrum 2 (Patthi and Awang, 2011)

produce enough heat which causes phase changes within the material due to the onset of melting and re-solidification. D-spacing analysis (Table 1) also indicates an insignificant amount of changes in the weld space lattice due to the onset of plastic deformation but the slight increase in d-spacing value does indicate a slight expansion stress (HAZ and weld nugget). Results from Table 1 shows the highest space lattice distortion (d spacing) in the TMAZ especially in the aluminum peaks of about 2.31261 nm which shows the occurrence of compression. This compression is due to centrifugal force during the stirring action, which induces some stresses within the material matrix.

EDX analysis: EDX analysis was further implemented on the welded sample. Spot EDX was implemented to identify different elements on the cross section of the weld, Fig. 6a. It was confirmed that bright particulate scattered across the micrograph were the SiC particulate (Fig. 6b), while the greyish matrix is confirmed to be the aluminium matrix (Fig. 6c).

Temperature analysis: It is also important to take notice the influence of heat in friction stir welding. Heat which was signified by earlier experimental work could influence the size of the grain boundaries, residual stress and ultimately the strength of the material. In addition the

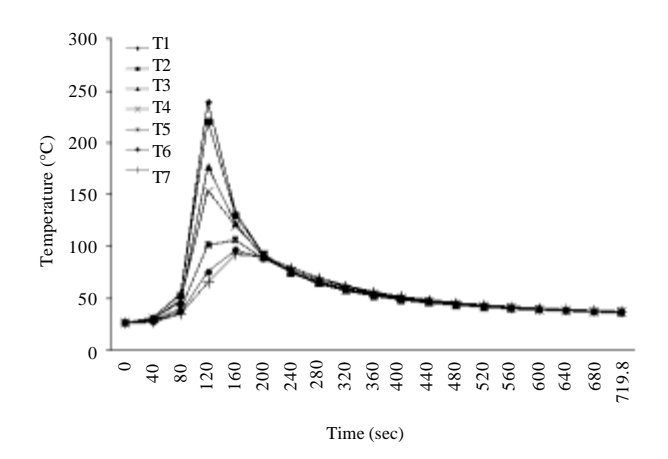


Fig. 7: Temperature vs. time graph at 7 different points during FSW

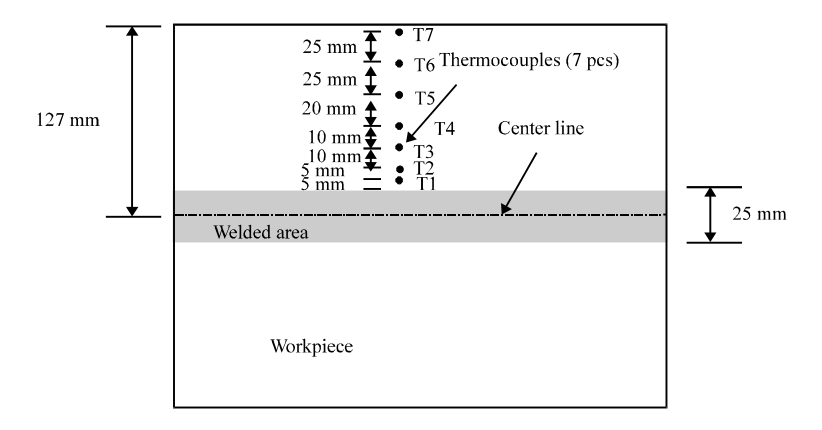


Fig. 8: Placement of thermocouple on the welded plate

working temperature could greatly influence the performances and efficiency of the welding process itself. A too low working temperature could cause an increase in the liquid viscosity which could damage the probe but a too high working temperature could probably causes the material to coat the tool and an increase in temperature could also causes changes in the material phases and properties (Hwang *et al.*, 2008).

A thermal history was recorded during the FSW on the aluminum composite plates which is shown in Fig. 7. Seven points perpendicular to the welding line that is in the Retreating Side (RS) were selected and thermocouple probes were inserted or imbedded into the seven points. The points were stack up on the same welding location with different distances between one another which can be viewed in Fig. 8. T1 is located to the closest point to the welding line which is then continued to T2 and so on. An even behaviour of the temperature distribution was exhibited between the seven points during the lateral movement of the tool, which marks the highest temperature recorded for the seven points approximately at 104 sec.

The maximum working temperature recorded was about 355°C at T1 which is fairly near the ideal working temperature for the aluminium alloy matrix which is between 365-390°C

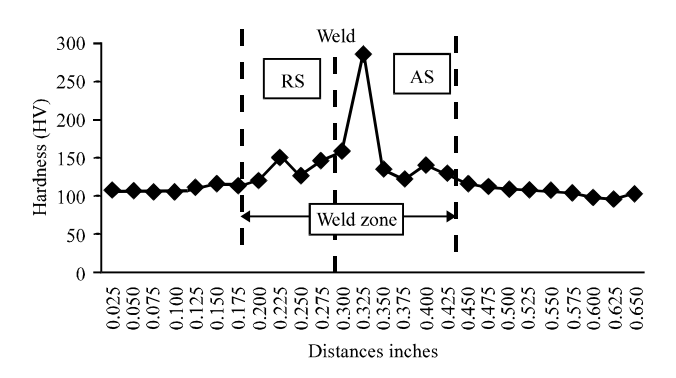


Fig. 9: Micro hardness profile measured across the cross section of the friction stir welded 6092+25%

Table 2: Tensile test of un-welded and welded samples

| Sample | UTS (MPa) | Elongation (%) |
|-----------------|-----------|----------------|
| Un-welded plate | 266.54 | 2.884 |
| Welded plate | 256.62 | 0.330 |

(Hwang *et al.*, 2008). No SiC decomposition or melting of the aluminum matrix will take place at such working temperature. Complete SiC decomposition will take place approximately at 1727°C (Storjohann *et al.*, 2005).

Hardness test: The measured hardness in Figure 9 shows an increasing hardness trend when approaching the Advancing Side (AS) of the weld nugget from the Retreating Side (RS). This is partly due to the unsymmetrical distribution of coarse and fine SiC particulate within the weld nugget which is due to difference in stirring rate. It can be seen that the weld nugget hardness is higher than the base metal which confirm previous work done on this topic (Govindaraju *et al.*, 2012). Average hardness of the weld nugget is 140 HV while average hardness of the base metal is 105 HV.

Tensile test: The result from Table 2 shows an adequate retainment of the material properties. Tensile result shows that there was an adequate retention of ultimate tensile strength (UTS) in the welded sample from 266.54 MPa to 256.62 MPa but a sharp decrease in the material elongation to failure when compared to the base material. Approximately there was a decrease of about 2.6% in elongation to failure in the welded plate when compared to the un-welded plate.

CONCLUSION

There are several conclusions that can be made from the above analyses. The micrograph analysis shows changes in the SiC particulate orientation and concentration within the aluminum matrix due to the stirring action. A higher concentration of fine SiC particulate was detected in the advancing side when compared to the weld centre and retreating side. The retreating side shows a lesser density of fine SiC particulate and denser coarse SiC particulate when compared to the advancing side. XRD result shows no formation of additional phases which concludes retained material chemical properties after the welding process. The XRD results also indicate changes in the lattice space between the regions especially in the TMAZ about 0.01 nm when compared to the base metal. Insignificant amount of changes in d-spacing were detected between the welded zone

and the base metal. Vickers hardness reading indicates an average of 140 HV in the weld nugget when compared to an average hardness of 105 HV in the base metal. Hardness test also shows higher hardness reading in the advancing side of the weld when compared to the retreating side. Tensile test shows an adequate retained material ultimate tensile strength of about 256.62 MPa but steep reduction in the material elongation to failure of about 2.6%. The recorded maximum working temperature is 355°C which indicates that processes were working well in the reaches of standard or nominal working temperatures.

ACKNOWLEDGMENT

This study has been supported by the Universiti Teknologi PETRONAS under STIRF code number of 43/09.10.

REFERENCES

- Awang, M., I.M. Ahmat and P. Hussain, 2011. Experience on friction stir welding and friction stir spot welding at Universiti Teknologi PETRONAS. J. Applied Sci., 11: 1959-1965.
- Govindaraju, M., J. Kandasamy, M. Manzoor Hussain and K. Prasada Rao, 2012. Some aspects of cross butt friction stir weldments of rare earth magnesium alloys: Novel attempts in friction stir welding. J. Applied Sci., 12: 1043-1047.
- Hwang, Y.M., Z.W. Kang, Y.C. Chiou and H.H. Hsu, 2008. Experimental study on temperature distributions within the workpiece during friction stir welding of aluminum alloys. Int. J. Mach. Tools Manuf., 48: 778-787.
- Maruyama, B., 1999. Discontinuously reinforced aluminum: Current status and future. JOM J. Miner. Met. Mater. Soc., 51: 59-61.
- Patthi, U.B. and M. Awang, 2011. Friction stir welding on aluminum 6092/SiC/25p/t6 metal matrix composite: Its microstructure evolution and mechanical properties. Proceedings of the National Postgraduate Conference, September 19-20, 2011, Kuala Lumpur, Malaysia, pp. 1-6.
- Root, J.M., D.P. Field and T.W. Nelson, 2009. Crystallographic texture in the friction-stir-welded metal matrix composite Al6061 with 10 vol Pct Al₂O₈. Metall. Mater. Trans. A, 40: 2109-2114.
- Storjohann, D., S.S. Babu, S.A. David and P. Sklad, 2003. Frictionstir welding of aluminum metal matrix composites. Proceedings of the 4th International Symposium on Friction Stir Welding, May 14-16, 2003, Utah, USA.
- Storjohann, D., O.M. Barabash, S.A. David, P.S. Sklad, E.E. Bloom and S.S. Babu, 2005. Fusion and friction stir welding of aluminum-metal-matrix composite. Metall. Mater., 36: 3237-3247.
- Uzun, H., 2007. Friction stir welding of SiC particulate reinforced AA2124 aluminium alloy matrix composite. Mater. Des., 28: 1440-1446.